Submission code: G96JYM859R

See this and other abstracts on our website: https://home.sbgf.org.br/Pages/resumos.php

Automated Analysis of Grain Size and Morphology in Petrograph Using Fourier Descriptors and Machine Learning

Victor Moreira (UFPA), Jose Jadsom Sampaio de Figueiredo (UFPA), Yana Carolina Pinheiro Machado (UFPA)

Automated Analysis of Grain Size and Morphology in Petrograph Using Fourier Descriptors and Machine Learning

Automated Analysis of Grain Size and Morphology in Petrograph Using Fourier Descriptors and Machine Learning

Please, do not insert author names in your submission PDF file.

Abstract

Grain shapes were characterized using Fourier series based on the radius around the center of mass from peripheral point coordinates. This method applies Fourier descriptors to digitized petrographic images. Preprocessing involved highlighting, segmentation, and contour extraction to isolate grains. Contours were uniformly sampled and represented by Fourier coefficients, minimizing issues related to centroid location and edge irregularities. Data were standardized for scale, rotation, and starting point. The discrete Fourier transform, applied via FFT, provided harmonic amplitudes whose moduli described shape features. Despite similar amplitude curves, discriminant analysis distinguished complex morphologies. The study combines theoretical foundations, methodological steps, and geotechnical applications, contributing to automation in petrographic analysis.

Introduction

The morphometric characterization of mineral grains is key to understanding the physical behavior of geological materials, influencing properties such as porosity, internal friction, and compaction (Ehrlich and Weinberg (1970); Mollon and Zhao (2012)). Grain shape and surface texture affect packing and mechanical strength, playing a critical role in sedimentological, petrophysical, and geotechnical analyses. Traditional geometric descriptors fall short in capturing the complexity of irregular grain morphologies. To address this, we propose using Fourier descriptors to represent grain contours through harmonic decomposition (Gonzalez and Woods (2002); Virtanen et al. (2020)). This enables multiscale quantification of roughness and angularity, even for complex shapes. Our methodology combines computer vision (Bradski (2000); van der Walt et al. (2014)), density-based segmentation (Ester et al. (1996)), fast Fourier transforms (Harris et al. (2020)), and machine learning (Pedregosa et al. (2011)) to extract, smooth, and analyze contours from petrographic images. This approach enhances automation and standardization in petrographic analysis, minimizing subjectivity and providing robust, quantitative insights into grain morphology for diverse geoscientific applications.

Methodology

Petrographic images were preprocessed using Python libraries such as OpenCV Bradski (2000), NumPy Harris et al. (2020), SciPy Virtanen et al. (2020), and Scikit-Image van der Walt et al. (2014). Grayscale conversion and binarization (threshold $>$ 155) were used to isolate grains. Smoothing was applied using a Gaussian filter Gonzalez and Woods (2002). Grain segmentation used the DBSCAN algorithm Ester et al. (1996) with `eps = 10` and `min_samples = 10`. Morphological operations (e.g., fill holes, remove small holes) removed artifacts and noise. Grain center of mass was computed to extract radial vectors $r(\theta)$. Fourier smoothing retained only the first H harmonics, selected by minimizing MSE. Spectral (Dn, Pjk) and geometric, Circularity, Roundness and Regularity (CI, RO, RE), descriptors were computed as in Mollon and Zhao (2012).

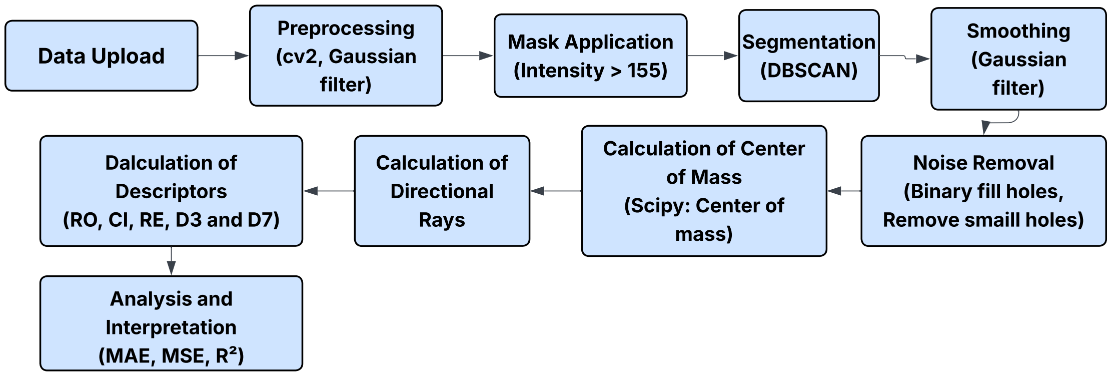

Figure 1: flowchart showing the steps taken in the methodology.

Results

Grains 8, 9, and 12 showed distinct morphological features. Grain 8 exhibited high angularity (D3=2.381), Grain 9 had high medium-scale roughness (D7=0.868), and Grain 12 presented an almost spherical shape (RO=0.898, CI=0.807).

Table 1: Morphological descriptors of the analyzed grains

Grain	D3	D7	RO	CI	RE	P2/P1	P3/P1
7	1.024	0.135	0.697	0.486	1.891	0.09	0.07
8	**2.381**	0.407	0.744	0.554	2.706	0.05	0.03
9	0.980	**0.868**	0.592	0.351	1.520	0.19	0.13
10	0.292	0.222	0.778	0.605	2.299	0.09	0.09
11	1.022	0.225	0.687	0.472	1.996	0.10	0.08
12	0.383	0.161	**0.898**	**0.807**	**3.681**	0.08	0.11

The geotechnical interpretation of morphological descriptors revealed that high angularity (D3 $>$ 1.0) is associated with greater mechanical interlocking between grains. Subrounded grains with low sphericity (RO $<$ 0.7) tend to reduce compaction efficiency, while non-spherical particles (CI $<$ 0.5) promote anisotropic load distribution. Additionally, high spectral roughness (P2/P1 $>$ 0.15) correlates with increased internal friction, impacting the mechanical stability of granular systems.

Table 1 presents the morphological descriptors of the analyzed grains, allowing the identification of relevant characteristics for understanding their behavior. Among the evaluated grains, grains 8, 9, and 12 stand out, each with particularities suggesting distinct implications.

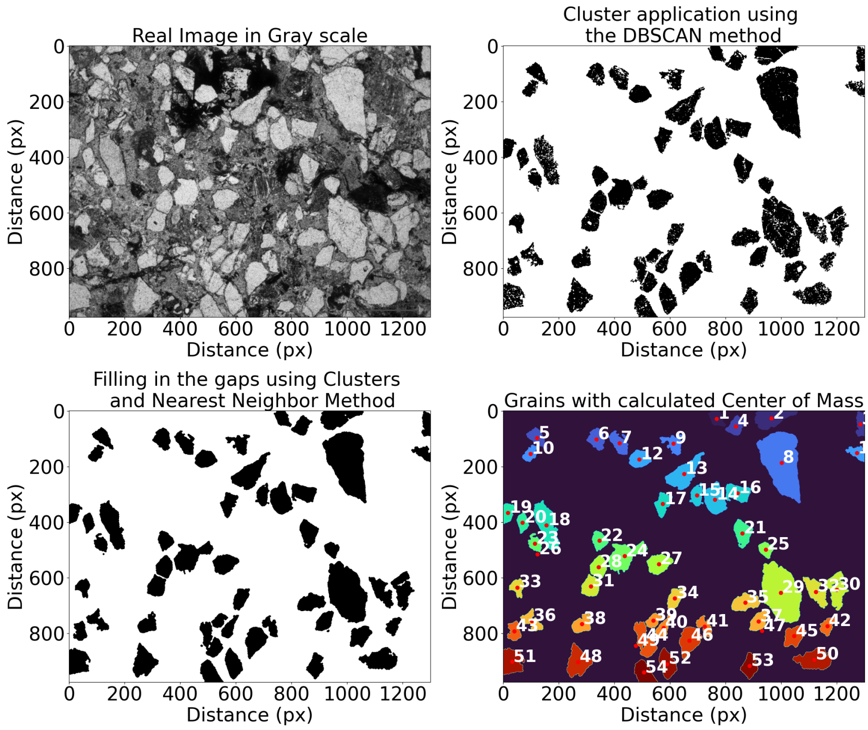

Figure 2: Original image after processing, masking, filtering and Result of calculating the center of mass in the image after filtering.

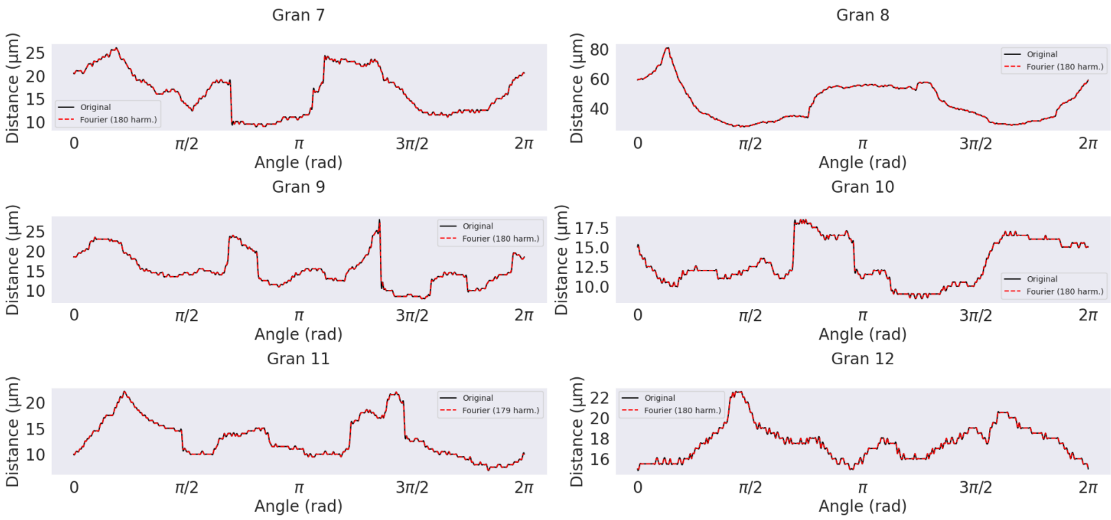

Figure 3: Graphs after grain tracking.

Grain 8 exhibits a significantly high D_3 value (2.381), which may indicate a highly angular geometry. This result could be due to a segmentation artifact, the presence of pronounced non-convex contours, or even an anomaly in the grain's shape that justifies this extreme measurement. Grain 9, on the other hand, stands out for its highest roughness ($D_7 = 0.868$) and lowest circularity (CI = 0.351) among all grains. These characteristics suggest a highly irregular surface and low sphericity, which may imply increased mechanical resistance to shearing, given the more complex contact between particles of this shape. Conversely, grain 12 shows the best performance in terms of shape, with high roundness (RO = 0.898), high circularity (CI = 0.807), and significant convexity (RE = 3.681). These values are characteristic of a near-spherical morphology, which is typical of more mature and well-reworked sediments, likely resulting in a more predictable and uniform granular behavior.

Conclusions

The morphometric and spectral analysis of grains 8, 9, and 12 using DBSCAN segmentation and Fourier-based smoothing revealed distinct differences in shape, texture, and structural complexity.

Grain 8 showed high angularity and moderate roughness, indicating a complex contour with concavities, yet a moderately rounded and globally convex shape—suggesting mechanical relevance in frictional systems. Grain 9 exhibited the highest roughness and low sphericity, with sharp undulations and high spectral ratios, pointing to a dense texture and high resistance to shear. In contrast, grain 12 was the most regular, with low angularity, high sphericity, and smooth contours, typical of mature sediments favorable for compaction and flow.

These results highlight the method's ability to capture subtle morphological variations, reinforcing the value of combining spectral and geometric descriptors for predicting the mechanical behavior of granular materials.

References

Bradski, G., 2000, The opencv library: Dr. Dobb's Journal, **25**, 120–126.

Ehrlich, R., and B. Weinberg, 1970, An exact method for characterization of grain shape: Journal of Sedimentary Petrology, **40**, 205–212.

Ester, M., H.-P. Kriegel, J. Sander, and X. Xu, 1996, A density-based algorithm for discovering clusters in large spatial databases with noise: Proceedings of the Second International Conference on Knowledge Discovery and Data Mining (KDD-96), AAAI Press, 226–231.

Gonzalez, R. C., and R. E. Woods, 2002, Digital image processing, 2nd ed.: Prentice Hall.

Harris, C. R., K. J. Millman, S. J. van der Walt, R. Gommers, P. Virtanen, D. Cournapeau, and T. E. Oliphant, 2020, Array programming with numpy: Nature, **585**, 357–362.

Mollon, G., and J. Zhao, 2012, Fourier-voronoi-based generation of realistic samples for discrete modelling of granular materials: Granular Matter, **14**, 621–638.

Pedregosa, F., G. Varoquaux, A. Gramfort, V. Michel, B. Thirion, O. Grisel, and E. Duchesnay, 2011, Scikit-learn: Machine learning in python: Journal of Machine Learning Research, **12**, 2825–2830.

van der Walt, S., J. L. Schönberger, J. Nunez-Iglesias, F. Boulogne, J. D. Warner, N. Yager, E. Gouillart, T. Yu, and the scikit-image contributors, 2014, scikit-image: Image processing in python: PeerJ, **2**, e453.

Virtanen, P., R. Gommers, T. E. Oliphant, M. Haberland, T. Reddy, D. Cournapeau, E. Burovski, P. Peterson, W. Weckesser, J. Bright, S. J. van der Walt, M. Brett, J. Wilson, K. J. Millman, N. Mayorov, A. R. J. Nelson, E. Jones, R. Kern, E. Larson, C. J. Carey, Polat, Y. Feng, E. W. Moore, J. VanderPlas, D. Laxalde, J. Perktold, R. Cimrman, I. Henriksen, E. A. Quintero, C. R. Harris, A. M. Archibald, A. H. Ribeiro, F. Pedregosa, and P. van Mulbregt, 2020, Scipy 1.0: Fundamental algorithms for scientific computing in python: Nature Methods, **17**, 261–272.